Geomechanics and Engineering, *Vol. 17, No. 1 (2019) 1-9*
DOI: https://doi.org/10.12989/gae.2019.17.1.001

Three-dimensional numerical modelling of geocell reinforced soils and its practical application

Fei Song[1a] and Yinghui Tian[*2,3]

[1]*Institute of Geotechnical Engineering, School of Highway Engineering, Chang'an University, Xi'an, 710064, China*
[2]*State Key Laboratory of Hydraulic Engineering Simulation and Safety, Tianjin University, 92 Weijin Rd., Nankai District, Tianjin 300072, China*
[3]*Ocean Graduate School, The University of Western Australia, 35 Stirling Highway, Crawley WA 6009, Australia*

(Received October 30, 2017, Revised November 19, 2018, Accepted November 23, 2018)

Abstract. This paper proposes a new numerical approach to model geocell reinforced soils, where the geocell is described as membrane elements and the complex interaction between geocell and soil is realized by coupling their degrees of freedom. The effectiveness and robustness of this approach are demonstrated using two examples, i.e., a geocell-reinforced foundation and a large scale retaining wall project. The first example validates the approach against established solutions through a comprehensive parametrical study to understand the influence of geocell on the improvement of bearing capacity of foundations. The study results show that reducing the geocell pocket size has a strong effect on improving the bearing capacity. In addition, when the aspect ratio maintains the same value, the bearing capacity improvement with increasing geocell height is insignificant. Comparing with the field monitoring and measurement in the project, the second example investigates the application of the approach to practical engineering projects. This paper provides a practically feasible and efficient modelling approach, where no explicit interface or contact is required. This allows geocell reinforced soils in large scale project can be effectively modelled where the mechanism for complex geocell-soil interaction can be explicitly observed.

Keywords: geocell; three-dimensional analysis; numerical modelling; foundation; retaining wall

1. Introduction

Geocell is one type of geosynthetic products, which are made of polymeric sheets interconnected by ultrasonically welded seams. It was originally developed by the US Army Corps of Engineers in 1970s for reinforcement of cohesionless soil in military field (Webster and Watkins 1977, Rea and Mitchell 1978, Webster 1979a, b). Due to its unique three-dimensional geometry, geocell can provide excellent lateral confinement to the infilled soil without relying on the interlocking or friction like the traditional geogrid. Geocell has been successfully used in various types of civil engineering projects, such as foundations, slopes and retaining walls, as a quick and effective technique for soil reinforcement. Fig. 1(a) and 1(b) show pictures of a typical geocell product and a retaining wall reinforced with geocell in a real project. The project shown in Fig. 1(b), which will be studied later in this paper, was used to protect a high embankment (50 m wide and 10 m high) for building an airport covering 2.89 km^2 with a total cost of $44 million dollars.

(a) Geocell products

(b) Geocell-reinforced retaining wall

Fig. 1 Examples of geocells

Despite the increasing popularity, numerical modelling geocell reinforced soils remains as challenging due to the complex interaction between the geocell membrane and the surrounded soil in three dimensional space. Unsurprisingly, most available studies in the literature tend to model the geocell and the encased soil as two-dimensional composite

∗Corresponding author, Professor
E-mail: yinghui.tian@tju.edu.cn
[a]Associate Professor
E-mail: songf1980@163.com

ISSN: 2005-307X (Print), 2092-6219 (Online)

material with equivalent strength and stiffness parameters (see among others, Bathurst and Knight 1998, Madhavi Latha and Rajagopal 2007, Madhavi Latha *et al.* 2008, 2009, Xie and Yang 2009, Chen *et al.* 2013, Mehdipour *et al.* 2013, Hegde and Sitharam 2013, Li *et al.* 2018 and 2019). This approach is only meaningful with retrospective fitted composite material property while it suffers from lacking the versatility to investigate the real failure mechanism of geocell reinforced soils.

The limited number of explicitly modelling the geocell and soil with contacts and interfaces found in the literature is summarized here. Han *et al.* (2008), Saride *et al.* (2009), Yang *et al.* (2010) and Hegde and Sitharam (2015a, b) conducted three-dimensional numerical analysis employing commercial package FLAC3D, an explicit finite difference program, to study the behavior of circular footing supported on geocell reinforced soil. In their analyses, the geocell was modelled using the in-built geogrid structural elements. The interfaces between the geocell and the soil were modelled with interface elements obeying Mohr-Coulomb criterion. The calculation models in their studies were all restricted to the scale of laboratory model tests presumably due to the challenges of computation efficiency with significant computation efforts to explicitly model the interface elements. In addition, the challenging coding work to seek the node connection between the geocell and the soil element in their analyses can be overly complicated for the daily work of engineers. Leshchinsky and Ling (2013a, b) carried out three-dimensional numerical simulation of railway ballasted foundation with geocell reinforcement employing the commercial finite element package, ABAQUS. In their study, the geocell was modelled as tetrahedral four-node solid elements while the interaction between geocell and infilled gravel was described with contact. It can be seen that explicitly modelling the geocell and soil with contacts and interfaces is not impossible to be done. However it is not practical nor efficient to do so as this method tends to consume significant amount of calculation time with the large number of continuum elements and contact interactions. This is especially the case when modelling a large scale project where unrealistic computation efforts of modelling numerous geocell pockets in three dimensional space prevents its wide application. More importantly, modelling geocell using continuum elements inevitably results in bending moments in the geocell, which is not consistent with the mechanical characteristics of flexible geocells in engineering practices.

In this paper, a new approach to model three dimensional geocell reinforced soil is developed based on finite element method. Geocell was described as three-dimensional, 4-node membrane elements, which are thin surface elements that transmit only in-plane forces. They do not have bending stiffness and cannot transmit moments, which well represents the behaviour of practical geocell material. No compression was allowed in the geocell material definition, which is to ensure that no compressive stresses occurring in membrane elements. This is expected to give more realistic representation of the membrane behavior. The interaction between the geocell and the soil is realised by specifying an element or a group of geocell elements embedded in a group of host soil elements. The host soil response will be used to constrain the translational degrees of freedom of the embedded geocell nodes. See Fig. 2 for illustration of the idea. In the computation, the geometric relationships between nodes of the embedded geocell elements and the host soil elements are searched. If a node of an embedded geocell element lies within a host soil element, the translational degrees of freedom at the embedded node are constrained to the interpolated values of the corresponding degrees of freedom of the host soil element. By coupling the degree of freedom of geocell and the surrounded soil, no complex contact or interface elements are required in this approach, which is essential to significantly improve the computation efficiency and to make simulation of large scale models becoming feasible and practicable.

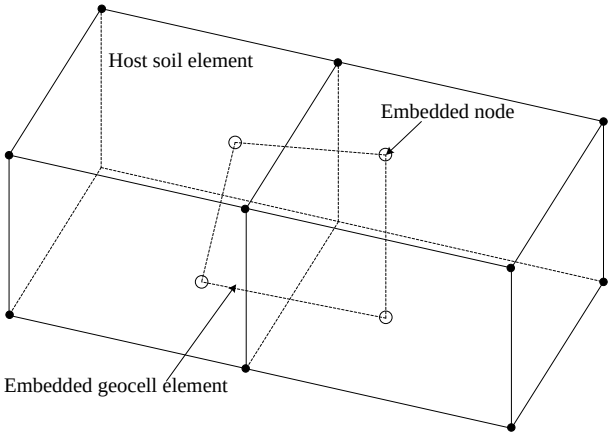

Fig. 2 Illustration of embed element constraint

In this paper, two examples are demonstrated using this approach. The first example studies the bearing capacity of a circular footing sitting on geocell-reinforced clayey soil. Based on validation against established solutions, this example aims to demonstrate this approach with a parametric study showing the influence of key geocell parameters. The second example simulates the geocell-reinforced retaining wall as shown in Fig. 1(b) compared with filed measurement and monitoring, which provides a practically feasible modelling approach to investigate the mechanism for complex geocell reinforced structures.

2. Bearing capacity of circular foundation on geocell reinforced soil

2.1 Finite element model

To take advantage of symmetry, a quarter of the model is considered as shown in Fig. 3, where D, h, u and b represent the diameter of the footing, the height of the geocell, the depth to the top of the geocell layer from the base of the footing, the width of geocell layer, respectively. The geocell pockets are in a square shape mimicking the operation condition and the side length of the square is denoted with a. The circular footing is modelled as a rigid body and with a diameter of D=2 m. The height of the soil domain is taken as 5D and the width of the soil is 3D. A model size and mesh sensitivity study was carried out, where the model used in this study (soil height 5D, soil width 3D) can effectively eliminate the boundary influence.

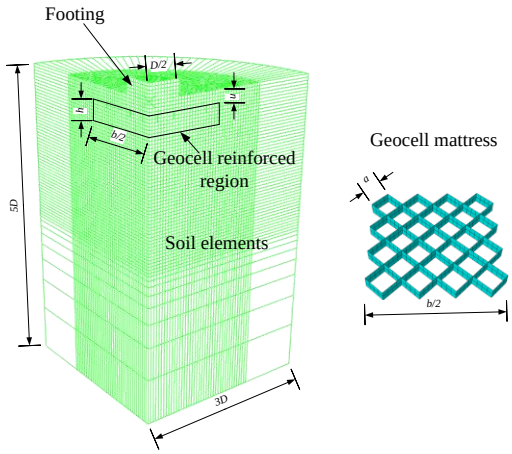

Fig. 3 Mesh of the calculation model

Table 1 Calculation cases

Calculation series	Depth to the top of the geocell	Height of geocell	Side length of geocell pocket	Width of geocell layer	Number of geocell layers
	u	*h*	*a*	*b*	*n*
Base case	0	0.1*D*	0.2*D*	2.26*D*	1
Case A	0, 0.1*D*, 0.2*D*, 0.25*D*	0.1*D*	0.2*D*	2.26*D*	1
Case B	0	0.05*D*, 0.1*D*, 0.15*D*,0.2*D*	0.2*D*	2.26*D*	1
Case C	0	0.1*D*	0.05*D*, 0.1*D*, 0.15*D*, 0.2*D*, 0.25*D*	2.26*D*	1
Case D	0	0.1*D*	0.2*D*	1.13*D*, 1.70*D*, 2.26*D*, 2.83*D*, 3.39*D*, 3.96*D*	1
Case E	0	0.1*D*, 0.075*D*, 0.05*D*	0.2*D*, 0.15*D*, 0.1*D*	2.26*D*	1
Case F	0	0.1*D*	0.2*D*	2.26*D*	1, 2, 3, 5,8 , 10

This soil domain size agrees with the practice of Griffiths and Fenton (2001), Gourvenec and Randolph (2003), Cassidy *et al.* (2013). Further, the model mesh used in this study represents a good balance between accuracy and efficiency.

The soil domain is meshed using a structured pattern mesh with 67150 hexahedral eight-noded elements, which use selectively reduced integration technique to avoid volumetric locking. Fine mesh (with smallest element size of *D*/20) is used close to the footing and the meshing setup was proven to be appropriate from a mesh sensitivity study. The soil is modelled as elastic-plastic Mohr-Coulomb material and the properties are: unit weight γ=18 kN/m^3, Young's modulus E=35 Mpa, Poisson's ratio ν=0.49 (a value to approximate no volume change in undrained condition while to keep numerical stability), cohesion (undrained shear strength) c=30 kPa, friction angle φ=0 (modelling the undrained behavior). It is noteworthy that E does not influence the calculation results of the ultimate undrained bearing capacity. Adopting a large Young's modulus in this analysis intends to reduce the displacement required to fully activate the bearing capacity. Although geocells tend to be more economical to use in soft soils (with undrained shear strength less than 15 kPa), the engineering practices normally adopt replacing the soft and weak soils with stronger in-filling materials. Thus, c=30 kPa in this example is a reasonable estimation of the foundation. Following Han *et al.* (2008), Leshchinsky and Ling (2013a, b), Hegde and Sitharam (2015a, b), the geocell is modelled as elastic material with unit weight γ=9.5 kN/m3 and E=500 Mpa in this study. Poisson's ratio of geocell was taken as 0 to avoid the transversal compression stress when the geocell is pulled in one direction This is to reflect the feature that the geocell can only bear tensile force while cannot bear compression. It is noted that Monroy Aceves *et al.* (2010) dealt with the problem in a similar way.

A computation case without reinforced geocell was conducted to validate the model against the established solution (Cox *et al.* 1961, Houlsby and Wroth 1983, Martin 2001). A computation case named as 'base case' was carried out with computation parameters set as h/D=0.1, b/D=1.13, a/D=0.2, u/D=0, n=1, where n is the number of the geocell layers (see Fig. 3 for the meaning of other symbols). In order to investigate the influence of geocell parameters on the bearing capacity, 6 series of analysis cases (A-F) were carried out as listed in Table 1. Serial A is to study the influence of the depth of the geocell layer from the base of the footing, *u*. Serial B focuses on the effect of height of the geocell *h*. In Serial C, the effect of the geocell side length *a* is studied and Serial D is to investigate the geocell mattress width b. In Series E, *h*/*a* maintains as a constant while *h* and *a* are changed to study the influence on the bearing capacity. Series F studies the effect of geocell layer number *n*.

2.2 Results and discussions

Fig. 4 shows the relationship between normalised load Q/cA and normalised settlement s/D, where Q is the load acting on the footing, c is the cohesion of the soil, A is the area of the circular footing, s is the settlement of the footing and D is the diameter of the circular footing. The calculated bearing capacity factor, i.e., the ultimate value of Q/cA, of the unreinforced case is 6.13, which is only 1% greater than the exact solution of 6.05 derived from limit solutions (Cox *et al.* 1961, Houlsby and Wroth 1983, Martin 2001), showing the effectiveness and accuracy of the model in this study is acceptable. Fig. 4 indicates the bearing capacity for the geocell-reinforced foundation is larger than that of the unreinforced case, obviously showing that the geocell reinforcement increases the load-carrying capacity (or in other words reduces the footing settlement under certain load).

It can be observed from Fig. 4(a) that the bearing capacity of the geocell-reinforced foundation increases with the decrease of the distance between the top of the geocell layer and the base of the footing, u/D, which is straightforward to understand as the farther away of geocell

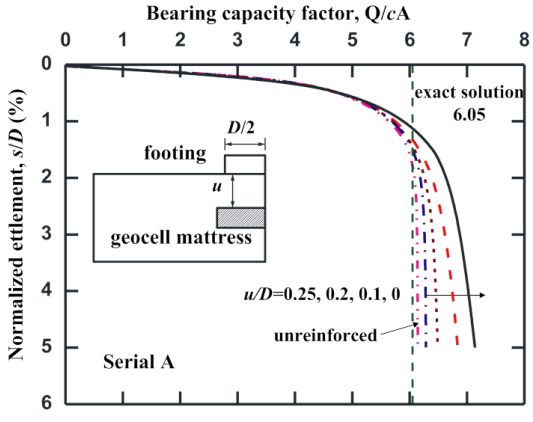

(a) Variation of bearing pressure with footing settlement for geocell mattress at different depths

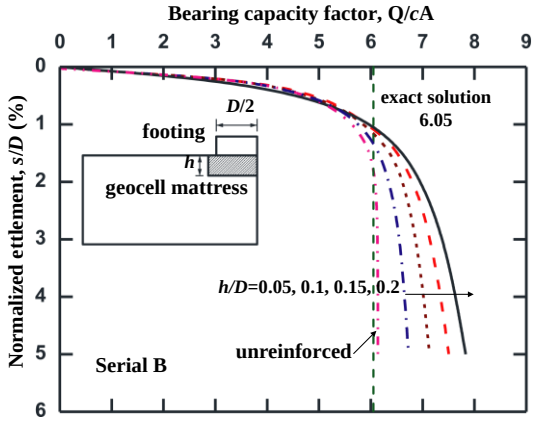

(b) Variation of bearing pressure with footing settlement for different heights of geocell mattress

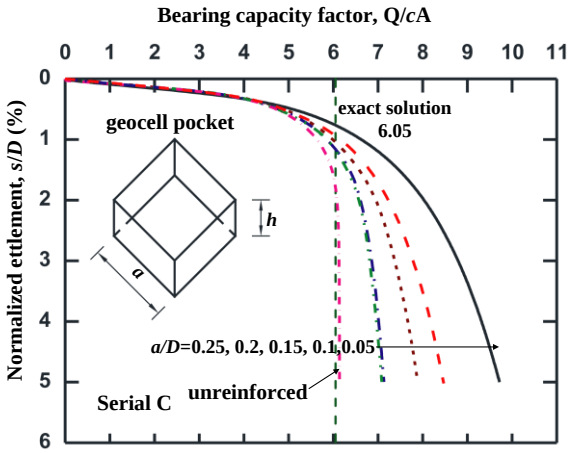

(c) Variation of bearing pressure with footing settlement for different geocell pocket size

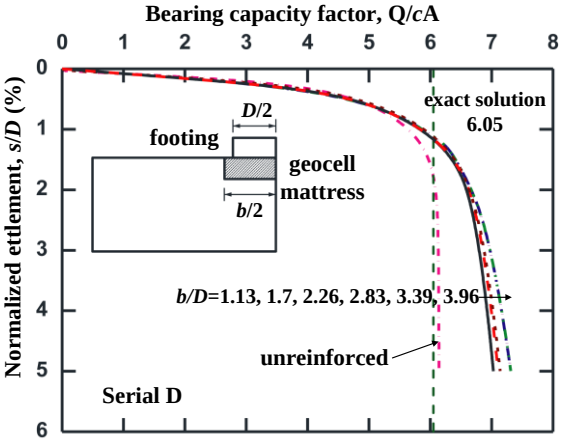

(d) Variation of bearing pressure with footing settlement for different widths of geocell mattress

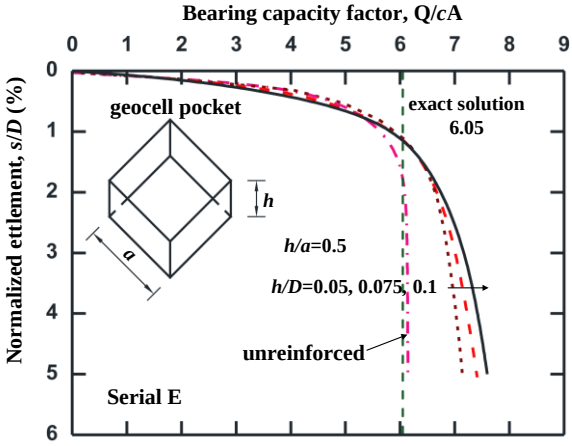

(e) Variation of bearing pressure with footing settlement for geocell mattress with h/a=0.5

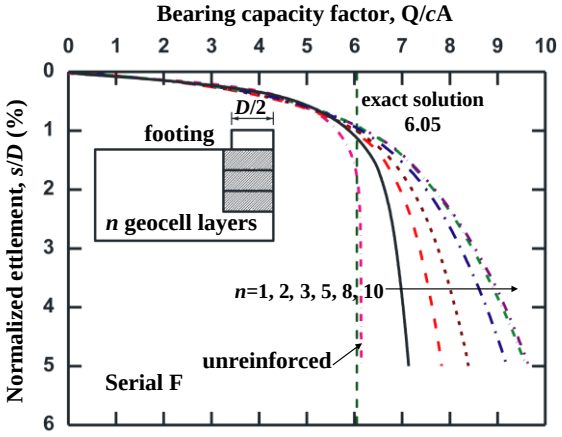

(f) Variation of bearing pressure with footing settlement for different number of geocell layers

Fig. 4 Computation results of surface footing

from footing, the less contribution it can do to the bearing capacity. This is consistent with the findings of Sitharam *et al.* (2005). At a settlement of s/D=5%, the bearing capacity of case u=0 is improved by 16% compared with the unreinforced case.

Fig. 4(b) shows the variation of bearing capacity with varying height h/D of geocell mattress. The bearing capacity increases with the increase of h/D, which is easy to understand as higher geocell mattress contributes more to the bearing capacity. This is consistent with the study results of Dash *et al.* (2003), Sitharam and Sireesh (2005) and Sitharam *et al.* (2005). At the settlement s/D=5%, the bearing capacity of case h=0.2D improved 28% compared with the unreinforced case.

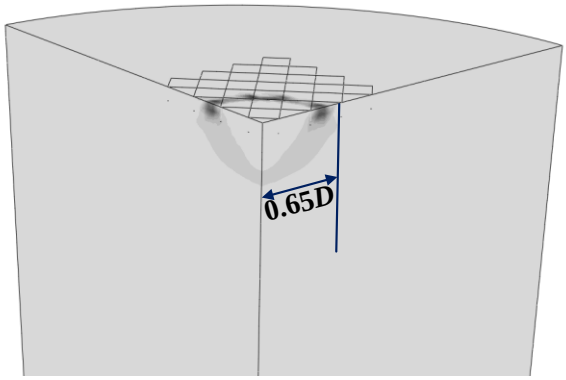

Fig. 5 The equivalent plastic strain and shear band

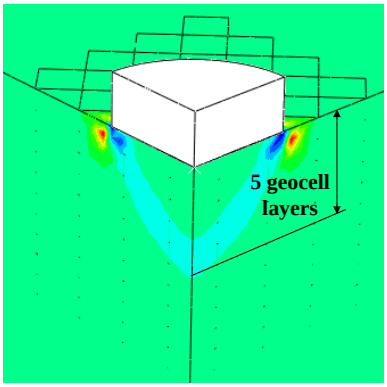

Fig. 6 The depth of plastic zone and failure mechanism

It can be observed that from Fig. 4(c) that the bearing capacity increases significantly with the reduction of the side length of the geocell pocket *a*. It is noted that the geocell width *b* was kept constant in this case. The smaller geocell pocket, i.e., denser pockets in unit area, provides stronger confinement to the encapsulated soil, which explains the increase of the bearing capacity. The bearing capacity of case a=0.05D improved 58% compared with the unreinforced case at s/D=5%. It can be seen that reducing the geocell pocket size *a* has a strong effect on improving the bearing capacity although more geocell material is required. There may exist an optimal side length *a* with a balance between capacity improvement and material usage for specific soil conditions.

It can be observed from Fig. 4(d) that the bearing capacity increases with the width of geocell mattress *b*. However, the bearing capacity improvement is not so significant for wider mattress (b/D=3.96) compared with b/D=1.13. This is believed due to the failure mechanism of the soil under surface footing are nearly confined with the range of b/D=1.13. Fig 5 shows the equivalent plastic strain plot as an illustration of the shear band and failure mechanism of the case of b/D=2.26. It can be observed from this figure that the shear band is contained within the range of b/D=1.3. It is thus understandable that capacity improvement by the geocell confinement is only marginal when the width of geocell mattress *b* is further increased.

It is very interesting that when the aspect ratio h/a (height *h* to side length *a*) maintains the same value, the bearing capacity improvement with increasing *h* is insignificant. The results are illustrated in Fig. 4(e). This implies that increasing geocell layer height *h* but increasing geocell pocket length *a* (loos pockets) only resulted in slightly increase of the bearing capacity. Similar finding was also reported by Krishnaswamy *et al.* (2000). At settlement of s/D=5%, the capacity improvement is around 21%.

It can be observed from Fig. 4(f) that the bearing capacity increases with the number of geocell layers n (i.e., the total height of geocell mattress is increasing). It is found that the bearing capacity of the case n=2 (with a total geocell mattress height of 0.2D) and a single layer with the height of 0.2D in Series B (Fig. 4b) are almost the same. It is noted that there is no direction interaction or constraints between different layers of geocell in the numerical analysis. This suggests that using multiple short layers can be equivalent to a single tall layer. From Fig. 4(f), the improvement of the bearing capacity is only marginal when the number of geocell layers is larger than 5 (the depth over 0.5D). This is thought due to the height of 5 geocell layers (0.5D) is comparable to the depth of plastic zone of the failure mechanism, as shown in Fig. 6. Thus, when $n\geq5$, the effect of geocell confinement is not so significant any more.

3. Simulation of geocell-reinforced retaining wall

3.1 Finite element model

Geocell-reinforced retaining wall has been used in engineering practices for the protection of embankments due to its advantages of reliability, aesthetics, economical cost, easy construction and good seismic performance. In this study, the geocell-reinforced retaining wall as shown in Fig. 1(b) was numerically modelled and compared with field observations. The dimension sketch of the project is shown in Fig. 7 with computation parameters and the three-dimensional finite element model is shown Fig. 8. Twenty one layers of geocell are infilled with loess, a kind of local soil in the North West part of China (see Qiu *et al.*, 2017 for more detailed introduction on this type of soil). Four strengthening geocell layers are infilled with cement sandy gravels and sandy gravels, which located at 0.33H, 0.5H, 0.74H and 0.9H from the wall bottom, wherein H is the height of the wall. The height h and the side length a of the geocell pocket are 0.2 m and 0.4 m, respectively. The length of the geocell layers are as shown in Fig. 7. A inclinometer tube and four earth pressure cells (located at 0.06H, 0.52H, 0.78H and 0.92H, respectively) behind the wall back were installed to measure the horizontal deformation and the horizontal earth pressures respectively (Fig. 7). The soil and the geocell are modelled in a similar way as the previous example where the calculation parameters are shown in Fig. 7.

The total length and height of the retaining wall are 50 m and 10 m (Fig. 1(b)). To reduce computation efforts of modelling the whole retaining wall, a slice of 1.7 m of the retaining wall is modelled (bearing in mind the geocell pocket side length a=0.4 m and thus this model includes 3 pockets). In order to correctly represent the real boundary conditions of the geocell-reinforced retaining wall and the embankment, the side faces of the slice are restrained from

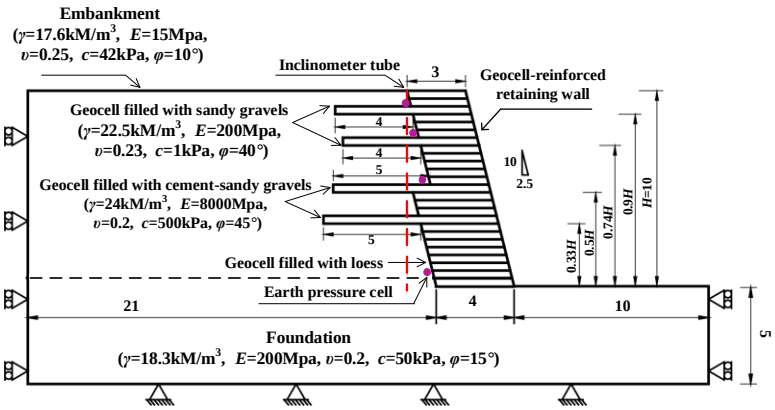

Fig. 7 Schematic diagram of the wall in a Chinese Airport Relocation Project (unit: m)

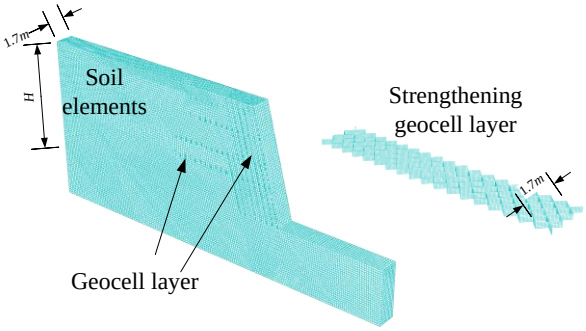

Fig. 8 Finite element model

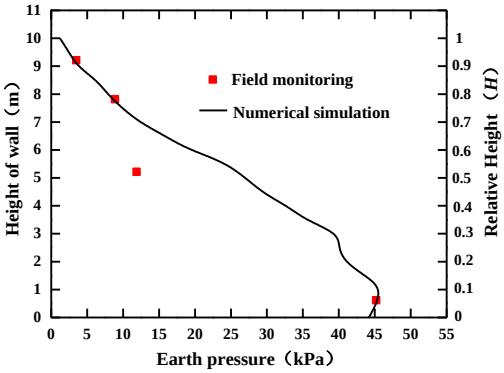

Fig. 11 Comparison of calculated earth pressure with the measured one

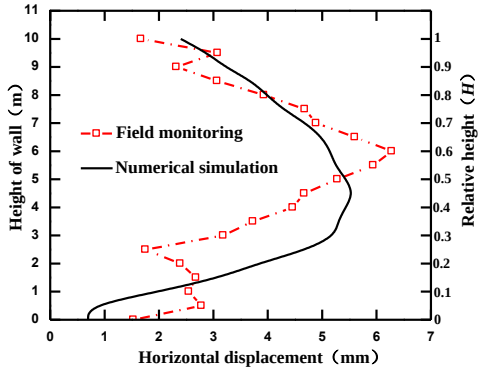

Fig. 9 Comparison of calculated horizontal displacement with the measured one

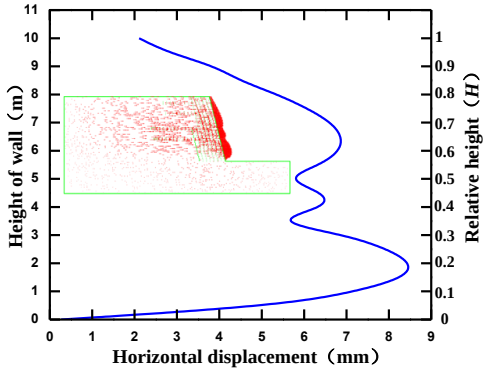

Fig. 10 Horizontal displacement of the slope surface

moving laterally but allowed to move vertically, i.e., symmetric plane constraint. The finite element model has 93078 hexahedral eight-noded solid elements (C3D8) and 232800 quadrilateral four-noded membrane elements (M3D4), which was proved to be a good balance between accuracy and efficiency from a mesh sensitivity study.

3.2 Results and discussions

The calculated horizontal deformation behind the back of geocell wall (the vertical plane along the inclinometer tube as shown in Fig. 7) is compared with the field measurement as shown in Fig. 9. It can be observed that the numerical predicted maximum horizontal displacement of the soil along the vertical plane is 5.5 mm (about 0.6‰*H*), which occurs at the location of 0.45*H* from the bottom of the wall. The field monitoring results show the maximum displacement is 6.3 mm occurring at the location of 0.6*H* from the bottom of the wall. The numerical model over estimates the horizontal displacements at the lower half part of the vertical plane. This reason for this over prediction has not been fully understood. Considering this complex three-dimensional problem, however, the numerical prediction is believed to be in fairly good agreement with the field measurement.

The horizontal displacement of the slope surface obtained from numerical simulation is shown in Fig. 10. The displacement vector plot is shown as inset. It can be seen the horizontal displacements mainly occur in the slope but not in the foundation. The maximum displacement is

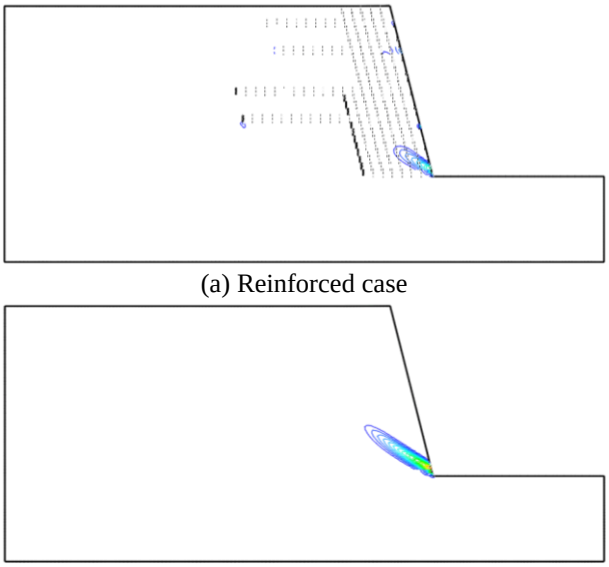

(a) Reinforced case

(b) Unreinforced case

Fig. 12 Shear band development

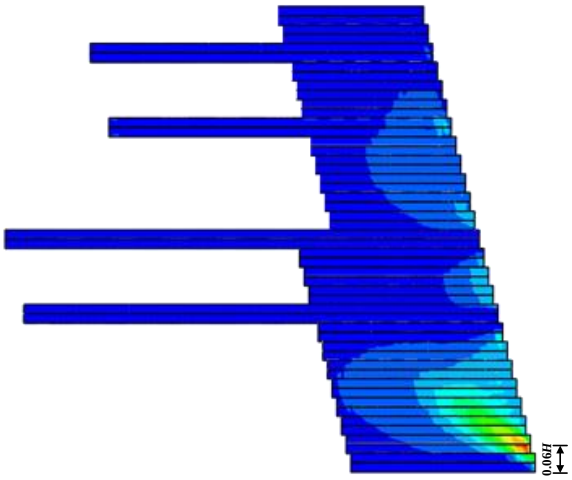

Fig. 13 Tensile strain distribution in the geocell layers

8.4 mm occurring at the location of 0.18*H* from the bottom of the wall. Because of the strengthening effect of the geocell layers filled with cement-sandy gravels at the place of 0.33*H* and 0.5*H* from the wall bottom, the horizontal displacement at these two locations decreases drastically, which can be seen from Fig.10.

The comparison of the calculated earth pressures against the geocell wall back and the measured values from the earth pressure cells is illustrated in Fig.11. It can be observed that the predicted earth pressure is in excellent agreement with the field measurements except the measurement of the second pressure cell (at 0.52*H*) from the bottom of the wall. It is difficult to judge whether the difference is from the inaccuracy or misbehavior of this pressure cell or the over prediction of the numerical model as there is quite limited data points available.

The total contour plot of the equivalent strain is shown in Fig. 12, where can be seen as the shear band development in the slope. Another case was conducted where no geocell is included. This figure clearly demonstrates that the geocell reinforcement effectively reduced the shear band development and thus improved the slope stability.

The horizontal tensile strain distribution in the geocell layers is illustrated in Fig. 13. The maximum tensile strain (0.28%) occurs around 0.06*H* from the bottom of the wall. Corresponding to the strain, the maximum tensile stress is 1.84 MPa occurring around the same place, which is within the yield strength of plastic geocell material (~20 MPa) and the junction peeling strength between geocell pockets (~10 MPa). The tensile strain in the geocell layers at the place of about 0.33H and 0.5H from the wall bottom are very small due to the strength of the cement-sandy gravels filled in these two layers is very high resulting in small tensile stresses in the geocell. Therefore, it is recommended that stronger geocell with high strength and stiffness can be used in the lower part of the wall to increase the stability of the retaining wall.

It is noted that this three dimensional computation model has 93078 soil elements and 232800 membrane elements. This computation example consumed 55 minutes on a desktop computer. It is not practically feasible to run such a scale on a desktop computer using explicit interaction between geocell and soil. This running time is well acceptable for engineering design and it demonstrates the efficiency of the proposed approach. In addition, the 'embedded element' technique employed in the proposed method to simulate the interaction between the geocell and the soil does not require the complicated coding work to seek the node connection between the geocell and the soil element. Therefore, it is convenient for the daily work of engineers.

4. Conclusions

In this paper, a practical approach for three-dimensional numerical modelling of geocell reinforced soils is proposed. In the numerical simulation, geocell was modelled as three-dimensional, 4-node membrane element and the interaction between the geocell and the soil was realized by restraining the embedded geocell node degree of freedom with the hosted soil element. The bearing capacity of a circular footing on geocell-reinforced clay soil has been studied. The research results indicate that using multiple short geocell layers can be equivalent to a single tall layer. However, the improvement of the bearing capacity is only marginal when the number of geocell layers is larger than 5 in this study. Furthermore, the behavior of the geocell-reinforced retaining wall has been numerically simulated and the horizontal deformation and earth pressures were compared with field measurement and monitoring. The agreement of the calculated horizontal deformation and earth pressures with the measured values validates of the proposed method. The high efficiency of proposed method is considered to have great potential to be used in geotechnical applications.

This three-dimensional approach in this paper provides additional insights into geocell modelling with no intention to replace the current two-dimensional analysis. It is acknowledged that two-dimensional analysis with

equivalent soil parameters is still useful. However, the equivalent soil parameters (strength and modulus) are empirical based and require rigorous validations before confidently using in the modelling. In contrast, the tensile stress and strain of the geocell can be obtained with the geocell is explicitly modelled using this three-dimensional approach.

It is acknowledged that the geocell material is only considered as elastic material in this paper. The stress in this paper's two examples is reasonably small and the material can be considered in elastic range. One further work would be to consider the plastic behavior of the geocell material and using user defined material is seen to be a practical approach. An elasto-plastic constitutive relationship of geocell developed by the authors is to be implemented to carry out extensive numerical simulation in future study.

In addition, the junction between two geocell pockets may be a weak part of the geocell and its peeling strength probably influences the mechanical behavior of geocell-reinforced soil. This remains another question for further study.

Acknowledgements

A big part of this work was carried out while the first author was a visiting scholar at the University of Western Australia, with acknowledgements of the support of the Fundamental Research Funds for the Central Universities (No. 300102218202), the National Natural Science Foundation of China (Grant No. 51879183, 51890913), the Australian Research Council Discovery Project (DP180103314), Natural Science Foundation of Tianjin (18JCYBJC40600). Prof J. Chu from Nanyang Technological University is appreciated for his time in discussion.

References

Bathurst, R.J. and Knight, M.A. (1998), "Analysis of geocell reinforced-soil covers over large span conduits", *Comput. Geotech*., **22**(3-4), 205-219.

Cassidy, M., Uzielli, M. and Tian, Y.H. (2013), "Probabilistic combined loading failure envelopes of a strip footing on spatially variable soil", *Comput. Geotech*., **49**, 191-205.

Chen, R.H., Wu, C.P., Huang, F.C. and Shen, C.W. (2013), "Numerical analysis of geocell-reinforced retaining structures", *Geotext. Geomembranes*, **39**(8), 51-62.

Cox, A.D., Eason, G. and Hopkins, H.G. (1961), "Axially symmetric plastic deformation of soils", *Proc. Royal Soc. London Ser. A*, **254**, 1-45.

Dash, S.K., Sireesh, S. and Sitharam, T. G. (2003), "Model studies on circular footing supported on geocell reinforced sand underlain by soft clay", *Geotext. Geomembranes*, **21**(4), 197-219.

Gourvenec, S. and Randolph, M. (2003), "Effect of strength non-homogeneity on the shape of failure envelopes for combined loading of strip and circular foundations on clay", *Geotechnique*, **53**(6), 575-586.

Griffiths, D.V. and Fenton, G.A. (2001), "Bearing capacity of spatially random soil: the undrained clay Prandtl problem revisited", *Geotechnique*, **51**(4), 351-359.

Han, J., Yang, X.M., Leshchinsky, D. and Parsons, R.L. (2008), "Behavior of geocell-reinforced sand under a vertical load", *Transport. Res. Rec. J. Transport. Res. Board*, (2045), 95-101.

Hedge, A. and Sitharam, T.G. (2013), "Experimental and numerical studies on footings supported on geocell reinforced sand and clay beds", *Int. J. Geotech. Eng*., **7**(4), 346-354.

Hegde, A. and Sitharam, T.G. (2015a), "3-Dimensional numerical modelling of geocell reinforced sand beds", *Geotext. Geomembranes*, **43**(2), 171-181.

Hegde, A.M. and Sitharam, T.G. (2015b), "Three-dimensional numerical analysis of geocell-reinforced soft clay beds by considering the actual geometry of geocell pockets", *Can. Geotech. J.*, **52**(9), 1-12.

Houlsby, G.T. and Wroth, C.P. (1983), "Calculation of stresses on shallow penetrometers and footings", *Proceedings of the IUTAM/IUGG Seabed Mechanics*, Newcastle, U.K., September.

Krishnaswamy, N R., Rajagopal, K. and Madhavi Latha, G. (2000), "Model studies on geocell supported embankments constructed over a soft clay foundation", *Geotech. Test. J*., **23**(2), 45-54.

Leshchinsky, B. and Ling, H. (2013a), "Effects of geocell confinement on strength and deformation behavior of gravel." *J. Geotech. Geoenviron. Eng*., **139**(2), 340-352.

Leshchinsky, B. and Ling, H. (2013b), "Numerical modeling of behavior of railway ballasted structure with geocell confinement", *Geotext. Geomembranes*, **36**, 33-43.

Li, C., Ashlock, J.C., Cetin, B., Jahren, C.T. and Goetz, V. (2018), "Performance-based design method for gradation and plasticity of granular road surface materials", Transportation Research Record, 0361198118787372.

Li, C., Ashlock, J.C., White, D.J. and Vennapusa, P.K. (2019), "Mechanistic-based comparisons of stabilised base and granular surface layers of low-volume roads", *Int. J. Pavement Eng*., **20**(1), 112-124.

Madhavi Latha, G. and Rajagopal, K. (2007), "Parametric finite element analyses of geocell-supported embankment", *Can. Geotech. J.*, **44**(8), 917-927.

Madhavi Latha, G., Dash, S.K. and Rajagopal, K. (2008), "Equivalent continuum simulations of geocell reinforced sand beds supporting strip footings", *Geotech. Geol. Eng*., **26**(4), 387-398.

Madhavi Latha, G., Dash, S.K. and Rajagopal,K. (2009), "Numerical simulation of the behavior of geocell reinforced sand in foundations", *Int. J. Geomech*., **9**(4), 143-152.

Martin, C.M. (2001), "Vertical bearing capacity of skirted circular foundations on Tresca soil", *Proceedings of the 15th International Conference on Soil Mechanics and Geotechnical Engineering*, Lahore, Pakistan, December.

Mehdipour, I., Ghazavi, M. and Moayed, R.Z. (2013), "Numerical study on stability analysis of geocell reinforced slopes by considering the bending effect", *Geotext. Geomembranes*, **37**, 23-34.

Monroy Aceves, C., Mcmillan, A.J., Sutcliffe, M.P.F., Stronge, W.J., Choudhry, R.S. and Care, I.C.D. (2010), *Low-Speed Impact Damage in Hybrid 2D-Braided Composite Plates*, in *Recent Advances in Textile Composites*, DEStech Publications, Inc., 306-313.

Qiu, L.J., Hao, M.D. and Wu, Y.P. (2017), "Potential impacts of climate change on carbon dynamics in a rain-fed agro-ecosystem on the Loess Plateau of China", *Sci. Total Environ*., **577**, 267-278.

Rea, C. and Mitchell, J.K. (1978), "Sand reinforcement using paper grid cells", *Proceedings of the Symposium on Earth Reinforcement*, Pittsburgh, Pennsylvania, U.S.A., April

Saride, S., Gowrisetti, S., Sitharam, T.G. and Puppala, A.J. (2009), "Numerical simulation of geocell-reinforced sand and clay", *Ground Improv*., **162**(4), 185-198.

Sitharam, T.G. and Sireesh, S. (2005), "Behaviour of embedded

footings supported on geocell reinforced foundation beds", *Geotech. Test. J.*, **28**(5), 452-463.
Sitharam, T.G., Sireesh, S. and Dash, S.K. (2005), "Model studies of a circular footing supported on geocell-reinforced clay", *Can. Geotech. J.*, **42**(2), 693-703.
Webster, S.L. (1979a), "Investigation of beach sand trafficability enhancement using sand-grid confinement and membrane reinforcement concepts", Report 1, Sand Test Sections 1 and 2, Technical Report GL-79-20, Geotechnical Laboratory, US Army Corps of Engineers Waterways Experimentation Station, Vicksburg, Mississippi, U.S.A.
Webster, S.L. (1979b), "Investigation of beach sand trafficability enhancement using sand-grid confinement and membrane reinforcement concepts", Report 1, Sand Test Sections 3 and 4, Technical Report GL-79-20, Geotechnical Laboratory, US Army Corps of Engineers Waterways Experimentation Station, Vicksburg, Mississippi, U.S.A.
Webster, S.L. and Watkins, J.E. (1977), "Investigation of construction techniques for tactical bridge approach roads across soft ground", Technical Report S-77-1, U.S. Army Engineer Waterways Experiment Station, Vicksburg, Mississippi, U.S.A.
Xie, Y.L. and Yang, X.H. (2009), "Characteristics of a new-type geocell flexible retaining wall", *J. Mater. Civ. Eng.*, **21**(4),171-175.
Yang, X.M., Han, J., Parsons, R.L. and Leshchinsky, D. (2010), "Three-dimensional numerical modeling of single geocell-reinforced sand", *Front. Arch. Civ. Eng. China*, **4**(2), 233-240.

GC